Journal of Applied Electrochemistry **32**: 111–117, 2002.

Ternary alkali carbonate composition-oxygen solubility relationship under atmospheric and pressurized conditions – a utility model for MCFC

M. MOHAMEDI*, Y. HISAMITSU and I. UCHIDA
Department of Applied Chemistry, Graduate School of Engineering, Tohoku University, 07 Aramaki-Aoba, Aoba-Ku, Sendai 980-8579, Japan
*(*author for correspondence, e-mail: mohamed@est.che.tohoku.ac.jp)*

Received 26 June 2000; accepted in revised form 18 October 2001

Key words: MCFC, optimization, oxygen solubility, pressurization

Abstract

The effect of $O_2/CO_2 = 90/10$ gas mixtures under pressurized conditions on the diffusion resistance during oxygen reduction was investigated in carbonate melts of variable composition ranging from the eutectics Li–K, Li–Na to ternary Li–Na–K carbonate melts. It was found that pressurization reduced the diffusion resistance of the reactant species in all compositions investigated. This was ascribed to the increase in concentration of the reactive species in the electrolyte. Reaction order plots of Warburg coefficient versus the total pressure in binary melts showed that: (i) mixed diffusion of superoxide ions and CO_2 prevails in lithium rich carbonates, and (ii) mixed diffusion of peroxide ions and CO_2 predominates in potassium rich carbonates.

By means of a computerized statistical analysis of the results, a partial cubic model was found to describe the relationship between alkali carbonate compositions, pressure, and Warburg coefficient. The optimum alkali carbonate compositions are: (i) 0.283Li–0.373Na–0.344K with σ_{app} equal to 137.68 Ω cm^2 s$^{-0.5}$ at atmospheric conditions, and (ii) 0.390Li–0.355Na–0.255K with σ_{app} 87.53 Ω cm^2 s$^{-0.5}$ and 4.2 atm under pressurized conditions.

1. Introduction

The current development target in molten carbonate fuel cell (MCFC) technology is achieving a lifetime of 40 000 h, with the key limiting factor for this target being cathode stability. The state of art cathode is usually formed by the *in situ* oxidation and subsequent lithiation (which enhances the electronic conductivity) of presintered porous nickel plaques [1]. The MCFC uses a mixture of alkali carbonates for the electrolyte. During cell operation, the carbonate ions take part in the anode and cathode reactions according to the following:

Anode

$$H_2 + CO_3^{2-} \rightleftharpoons CO_2 + H_2O + 2\,e^- \tag{1}$$

Cathode

$$1/2\,O_2 + CO_2 + 2\,e^- \rightleftharpoons CO_3^{2-} \tag{2}$$

The ionic conduction in the MCFC is achieved by transporting carbonate ions from the cathode to the anode.

For more than two decades, the (62 + 38) m/o (Li + K)CO_3 eutectic has been the electrolyte of choice for MCFCs operating at 650 °C. The dissolution of NiO in this melt, during cell operation, is one of the major factors restricting cell life. The dissolved nickel ions diffuse from the cathode towards the anode and are reduced to metallic nickel by dissolved hydrogen from the anode side. The nickel deposits eventually form an electronic conductive chain in the matrix and cause short-circuiting between the cathode and the anode. To overcome the dissolution of nickel oxide, there are two approaches: (i) the development of alternative cathode materials or (ii) changing the alkali carbonate electrolyte composition.

With regard to the first approach, several alternative cathode materials have been considered such as $LiCoO_2$ [2], $LiFeO_2$ [3], perovskite $La_xSr_{1-x}CoO_3$ [4], Ni–Co [5], Li_2MnO_3, mixed oxides ($LiFeO_2$–$LiCoO_2$–NiO) [6], Ni-Ti [7], and Ni–Al [8]. However, further studies are necessary in order to optimize their composition and morphology, and to analyze their long-term stability in the carbonate melt.

Concerning the second approach, application of the (53 + 47) m/o Li/Na carbonate mixture is a better choice for the following reasons:

(i) NiO solubility is lower than that of the Li/K eutectic. This leads to better cathode stability and prolonged lifetime [9],

(ii) The conductivity of the Li/Na carbonate is approximately two times higher than that of the Li/K eutectic [10],

(iii) The volatility of sodium in the Li/Na carbonate eutectic is ten times less than that of potassium in the Li/K eutectic [11].

One of the drawbacks of the Li/Na melt is its chemical oxygen solubility, which is two times lower than with the Li/K carbonate eutectic [12]. This impairs the cathode kinetics of O_2-reduction due to mass-transfer limitations and lower cell performance. It is therefore essential to investigate other alternative alkali carbonate compositions.

We have collected data on oxygen reduction in various electrolyte compositions under conditions of O_2/CO_2:90/10 at 650 °C [13]. These data are unique in the sense that they were also obtained under pressurized conditions (up to 5 atm). In this paper, we show how these results may be understood from the viewpoint of oxygen speciation in the various electrolyte compositions investigated. We also report the use of a computerized statistical analysis method to find the relationship between the experimental variables (electrolyte composition and total pressure) and the response variable (diffusion resistance). Using the same model, an optimum electrolyte composition is also proposed, under atmospheric and pressurized conditions.

2. Experimental details

Melt purification, gas handling, and cell assembly have been described previously [14–16]. The working electrode was a gold flag (0.39 cm^2), which was fully immersed in the melt. The counter electrode was a coiled gold wire (1 mm dia., 15 cm length). The reference electrode was a gold flag quasi-reference. Electrochemical measurements were carried out in alkali carbonates of different electrolyte compositions. The working temperature was 650 °C and was monitored by an alumel–chromel thermocouple sheathed in an alumina protective tube. A cylinder of premixed $O_2/CO_2 = 90/10$ supplied by Sumitomo Seika Chemicals was used. The total pressure was varied from 1 to 5 atmospheres.

Impedance measurements were carried out with the aid of a 1260 Solartron frequency response analyser. The spectra were recorded at open-circuit potential using a superimposed voltage signal of 10 mV amplitude in the frequency range 1 Hz to 10 kHz.

3. Results and discussion

3.1. *Data of interest*

A large amount of work on the oxygen reduction in molten carbonates has been reported but the reaction mechanism is still unknown. Several species have been postulated to participate in the oxygen reduction mechanism. Many (electro)chemical equilibria among these species and amongst species constituting the melt have been presented. The predominant reaction mechanism depends on the gas composition and the temperature, as well as on the cationic composition of the electrolyte. In our previous work, the effect of O_2 and CO_2 partial pressures on oxygen reduction, at a gold flag electrode in (36 + 65) m/o (Li + K)CO_3, (62 + 38) m/o (Li + K)CO_3, (75 + 25) m/o (Li + K)CO_3, (52 + 48) m/o (Li + Na)CO_3, and (43.5 + 31.5 + 25.0) m/o (Li + Na + K)CO_3 melts, was analysed in the temperature range 615 to 800 °C [12]. It was concluded that the simultaneous diffusion of superoxide and carbon dioxide is the dominant feature of mass-transport associated with oxygen reduction in molten carbonate mixtures and, that of the two species, CO_2 diffusion is always the rate-limiting factor.

Under pressurized conditions of $O_2/CO_2 = 90/10$, impedance spectra revealed that oxygen reduction in Li–Na–K carbonate melts was mass-transfer limited, and that the impedance value depended both on the total pressure and the composition of the mixed carbonate melt [13]. Impedance spectra were modelled with a Randles-modified circuit, and the parameter of interest was the apparent Warburg coefficient σ_{app}, expressed as follows:

$$\sigma_{app} = \sum \frac{RT}{n_i^2 F^2 \sqrt{2}} \left(\frac{1}{C_i \sqrt{D_i}} \right) \tag{3}$$

where C_i is the concentration of the diffusing species i, and D_i its diffusion coefficient. Thus, a low value of σ_{app} would mean a low diffusion rate and, therefore, a high concentration of the electroactive species (if D_i is assumed constant). The Warburg coefficient derived from EIS measurements, at up to 5 atm pressure, is shown in Figure 1 for various electrolyte compositions. It can be seen that pressurization reduces the diffusion resistance of the reactant species in all compositions investigated. This is ascribed to the increase in concentration of the reactive species (Equation 3) in the electrolyte. Additionally, Figure 1 shows that lower σ_{app} are observed in some Li–Na–K carbonate compositions.

3.2. *Reaction order*

The most probable reaction mechanisms are summarized below [17–20]:

Peroxide mechanism (POP)

$$O_2 + 2\,CO_3^{2-} \overset{K_1}{\rightleftharpoons} 2\,O_2^{2-} + 2\,CO_2 \tag{4a}$$

$$\left[O_2^{2-}\right] = K_1 P_{O_2}^{0.5} P_{CO_2}^{-1.0} \tag{4b}$$

$$O_2^{2-} + 2\,CO_2 + 2\,e^- \rightarrow 2\,CO_3^{2-} \tag{4c}$$

Superoxide mechanism (SOP)

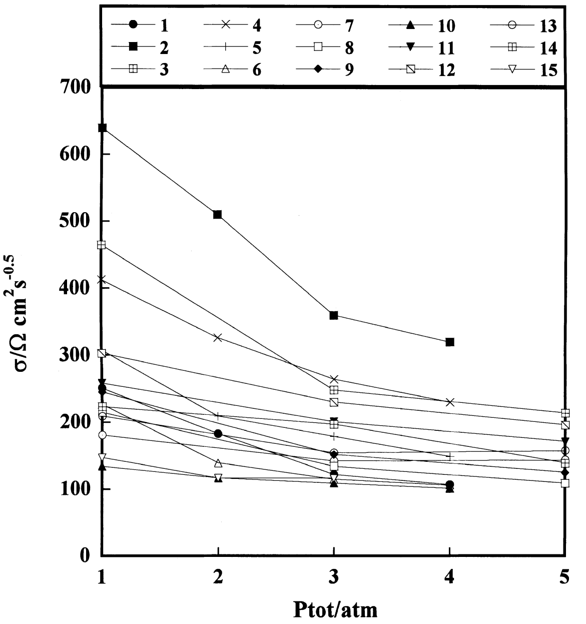

Fig. 1. Effect of the total pressure of O_2/CO_2 = 90/10 on Warburg coefficient at 650 °C in various Li–Na–K carbonate compositions. (1) 0.62–0–0.38, (2) 0.53–0.47–0, (3) 0.63–0.27–0.10, (4) 0.48–0.42–0.10, (5) 0.60–0.15–0.25, (6) 0.435–0.315–0.25, (7) 0.30–0.45–0.25, (8) 0.414–0.241–0.345, (9) 0.48–0.12–0.40, (10) 0.32–0.28–0.40, (11) 0.353–0.206–0.441, (12) 0.267–0.233–0.50, (13) 0.25–0.25–0.50, (14) 0.20–0.30–0.50, (15) 0.40–0–0.60.

$$3\,O_2 + 2\,CO_3^{2-} \overset{K_2}{\rightleftharpoons} 4\,O_2^- + 2\,CO_2 \tag{5a}$$

$$[O_2^-] = K_2 P_{O_2}^{0.75} P_{CO_2}^{-0.5} \tag{5b}$$

$$O_2^- + 2\,CO_2 + 3\,e^- \rightarrow 2\,CO_3^{2-} \tag{5c}$$

Percarbonate mechanism (PCP)

$$O_2 + 2\,CO_3^{2-} \overset{K_3}{\rightleftharpoons} 2\,CO_4^{2-} \tag{6a}$$

$$[CO_4^{2-}] = K_3 P_{O_2}^{0.5} \tag{6b}$$

$$CO_4^{2-} + CO_2 + 2\,e^- \rightarrow 2\,CO_3^{2-} \tag{6c}$$

The analysis of reaction order using Warburg coefficients was reported by Nishina et al. [12]. In the following, a similar method will be used to analyse the effect of pressurization on O_2 reduction.

By means of Equations 4(b), 5(b), 6(b), and for $[CO_2]$ expressed using Henry's law:

$$[CO_2] = K_H P_{CO_2} \tag{7}$$

the apparent value of σ_{app} may be expressed as a complicated function of P_{O_2} and P_{CO_2}. Nevertheless, if the following three limiting cases are applicable, the problem may be simplified.

I. Mixed diffusion of O_2^{2-} and CO_2

$$\sigma_{app} P_{CO_2} = A \times P_{CO_2}^{2} P_{O_2}^{-0.5} + B \tag{8}$$

II. Mixed diffusion of O_2^- and CO_2

$$\sigma_{app} P_{CO_2} = A \times P_{CO_2}^{1.5} P_{O_2}^{-0.75} + B \tag{9}$$

III. Mixed diffusion of CO_4^{2-} and CO_2

$$\sigma_{app} P_{CO_2} = A \times P_{CO_2} P_{O_2}^{-0.5} + B \tag{10}$$

A and B are positive coefficients that contain mass-transport parameters [12]. In cases I, II and III, it is assumed that only one reaction (i.e., POP, SOP and PCP, respectively) dominates the overall reaction. Thus, if any of these three limiting cases applies, it will show up as a linear dependence of the Warburg coefficient on the appropriate combination of powers of P_{O_2} and P_{CO_2}. Based on the above analysis, we have made reaction order plots for the Warburg coefficient, obtained at 650 °C under various total values of P_{O_2}/P_{CO_2} according to Equations 8–10, and the results are shown in Figures 2 and 3. For the sake of simplicity, only binary alkali carbonates were considered. The results show that:

(i) Case II (i.e., mixed diffusion of O_2^- and CO_2) is verified in lithium rich carbonates.
(ii) Case I (i.e., mixed diffusion of O_2^{2-} and CO_2) is verified in potassium rich carbonates.
(iii) Case III did not produce a linear dependence in any of the binary melts.

Concerning ternary electrolytes, linear relations were obtained for both cases II and I for all ternary compositions investigated (Figures 4 and 5). At this stage, it is difficult to explain these results. *In situ* Raman spectroscopy might help to further clarify the oxygen speciation in the ternary alkali carbonate melts. So far, we have succeeded in identifying superoxide ions in the

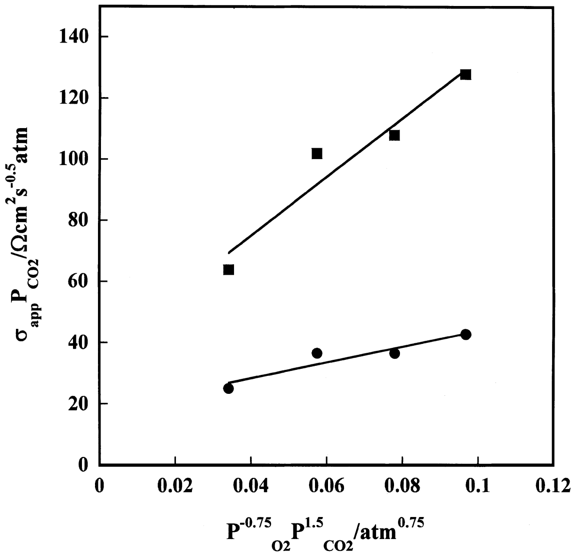

Fig. 2. Reaction order analysis of Warburg coefficients assuming mixed diffusion of superoxide ions and CO_2 in the binary electrolytes of (●) (62 + 38) m/o (Li + K) CO_3, and (■) (53 + 47) m/o (Li + Na) CO_3 at 650 °C.

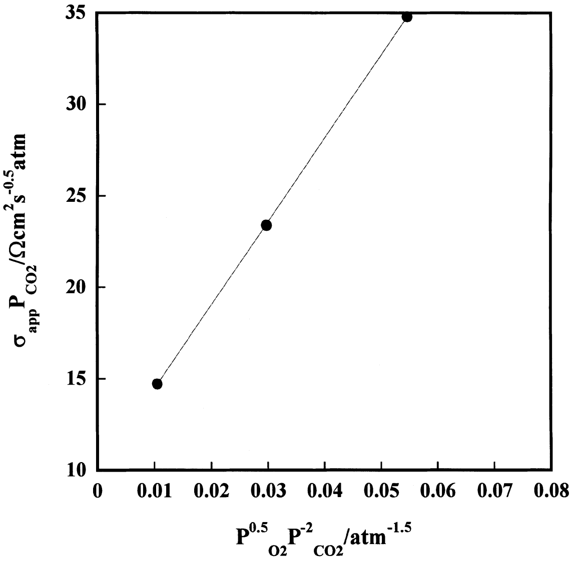

Fig. 3. Reaction order analysis of Warburg coefficients assuming mixed diffusion of peroxide ions and CO_2 in the binary electrolyte of (40 + 60) m/o (Li + K) CO_3 at 650 °C.

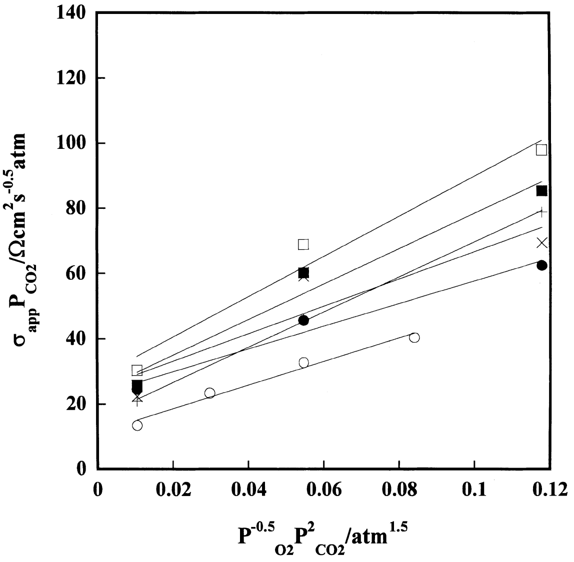

Fig. 5. Reaction order analysis of Warburg coefficients assuming mixed diffusion of peroxide ions and CO_2 in the ternary electrolytes of (●) 0.48–0.12–0.40, (○) 0.32–0.28–0.40, (■) 0.353–0.206–0.441, (□) 0.267–0.233–0.50, (+) 0.25–0.25–0.50, (×) 0.20–0.30–0.50 at 650 °C.

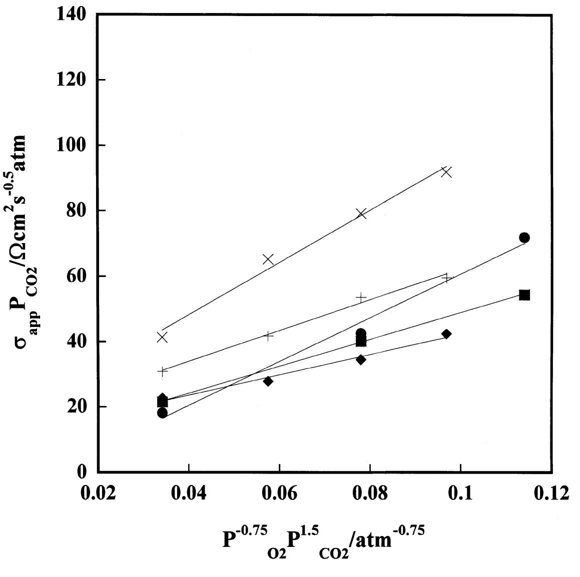

Fig. 4. Reaction order analysis of Warburg coefficients assuming mixed diffusion of superoxide ions and CO_2 in the ternary electrolytes of (×) 0.48–0.42–0.10, (+) 0.60–0.15–0.25, (◆) 0.435–0.315–0.25, (●) 0.30–0.45–0.25, and (■) 0.414–0.241–0.345 at 650 °C.

Li/K carbonate melt [21], and further studies are in progress in combination with different alkali carbonate compositions.

3.3. *Optimization of the electrolyte composition*

3.3.1. *Rationale*

The main goal is to discover the relationship between a response and one or more control variables. If y is a response, and $x_1, x_2, \ldots, x_p$ are a set of control variables, then one can suppose a functional relationship between the two, such as

$$y = f(x_1, x_2 \ldots x_p) \tag{11}$$

At the very least, such an equation can be used to predict values of y, for new combinations of the control variables. ECHIP™, a statistical experimental design program, was used to investigate the influence of electrolyte composition and total pressure on σ_{app}. A partial cubic model was utilized to analyse the response. A partial cubic model contains all the terms of a quadratic model plus terms involving cubic interactions. It does not contain pure cubic terms in a single variable. Since cubic interactions occur only rarely in chemical product development works, this exclusion is usually justified. As an example, for two variables, a partial cubic model is as follows:

$$\begin{aligned} y = {} & a_0 + a_1x_1 + a_2x_2 + a_{12}x_1x_2 + a_{11}x_1^2 + a_{22}x_2^2 \\ & + a_{112}x_1^2x_2 + a_{122}x_1x_2^2 \end{aligned} \tag{12}$$

where y represents the response σ_{app}, the term a_i and a_{ij} represent the estimations of the coefficients of the model and x_i are the control variables. In our notation, x_1, x_2, x_3 and x_4 designate Li_2CO_3, Na_2CO_3, K_2CO_3 and P (total pressure), respectively. x_1, x_2, and x_3 vary between 0 and 1, and the mixture of the three sums to unity.

The validity of the model was assessed both using the classical statistical tests of Box et al. [22] and the multiple correlation coefficient statistical (R^2). The R^2 value should be as close as possible to unity.

3.3.2. *Model adequacy*

The coefficient estimates of the model are displayed in Table 1. Figure 6 reports the 2D and 3D contour plots for the response surfaces. The limits of the convex hull are shown as straight lines forming polygonal shapes on

Table 1. Coefficients of the partial cubic model $y = f(x_1, x_2, x_3, P)$

Coefficients	Term
1053.91	constant
618.548	x_2
−579.946	x_3
−31.9568	P
−371.819	$x_1 \times x_2$
−720.828	$x_1 \times x_3$
−234.692	$x_1 \times P$
−152.22	$x_2 \times P$
398.831	$x_3 \times P$
935.629	x_1^2
994.586	x_2^2
1173.27	x_3^2
9.58812	P^2
−2448.1	$x_1 \times x_2^2$
−4586.8	$x_1^2 \times x_2$
−3959.74	$x_1 \times x_3^2$
−3373.67	$x_1^2 \times x_3$
29.6195	$x_1 \times P^2$
−103.408	$x_1^2 \times P$
−1259.49	$x_2 \times x_3^2$
−13169.2	$x_2^2 \times x_3$
144.029	$x_2^2 \times P$
−32.0064	$x_3 \times P^2$
−388.204	$x_3^2 \times P$

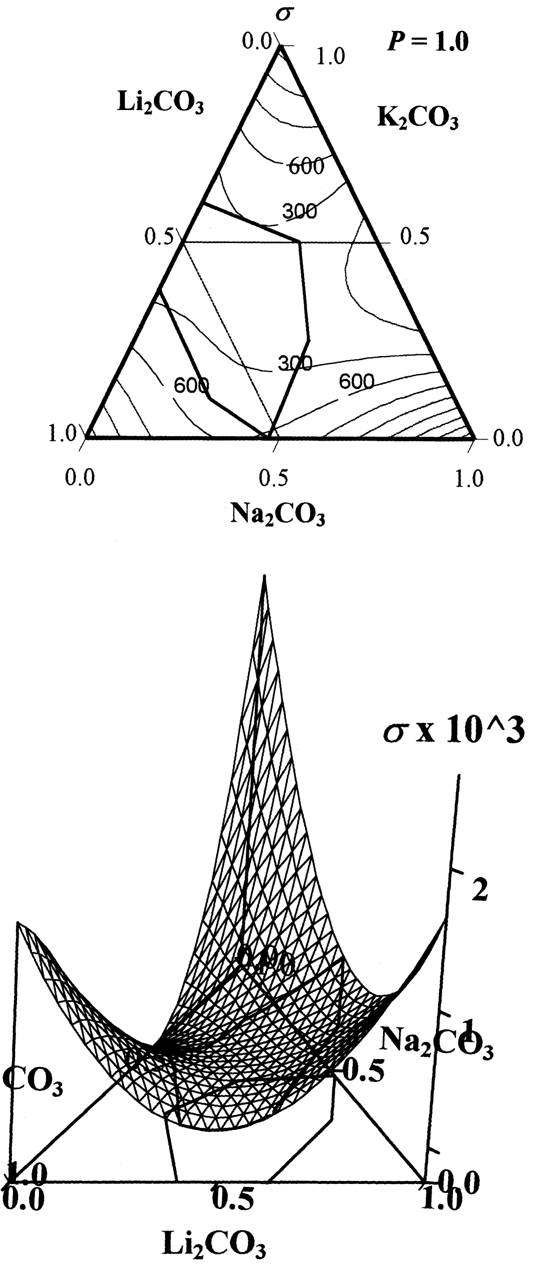

Fig. 6. Typical 2D and 3D response surface plots. y (σ_{app}) as function of alkali carbonates composition under $O_2/CO_2 = 0.9/0.1$ of 1 atm.

the plots. The convex hull is the minimum N-dimensional volume that contains all the trials for which the data have been collected. The plot of the fitted values versus the observed values is shown in Figure 7 with an excellent R^2 value of 0.965. Using standard plots one can assess data adequacy. In a plot of normal data against studentized residuals (errors standardized by distance from a central point within a distribution), the straight-line relationship implies that the errors (the disparity between what was expected and what was actually observed) are normally distributed (Figure 8).

3.3.3. *Optimization of electrolyte composition*

Before performing the optimization procedure, we first evaluated the predictive power of the model by selecting a new input of the electrolyte as 0.568Li–0.312Na–0.12K. Then, with the partial cubic model, values of σ_{app} at 1, 3 and 5 atm were predicted for the above carbonate composition. The experiments were then carried out at 650 °C for these pressures of $O_2/CO_2 = 90/10$ gas mixtures. Finally, σ_{app} was estimated by means of impedance spectroscopy and compared with the predicted σ_{app}. The results are shown in Table 2. All experimental values of σ_{app} are close to the predicted ones and fall within the upper and lower 95% confidence limits.

With ECHIP^{TM}, it is possible to optimize the response to a desired number, maximizing, minimizing (our interest), or requesting a specific target. The proper settings for the inputs and a guard band for the outputs, that yield the upper and lower 95% confidence limits, are generated by the software.

At 1 atm $O_2/CO_2 = 90/10$ and, within the scrutinized domain, a minimization procedure yields to a composition of 0.283Li–0.373Na–0.344K with σ_{app} equal to 137.68 Ω cm^2 s$^{-0.5}$. For comparison, the σ_{app} value for the ternary eutectic having the lowest melting point (397 °C) is 228.33 Ω cm^2 s$^{-0.5}$ at 0.435Li–0.315Na–0.250K.

Under pressurized conditions (1–5 atm), the optimum sets of conditions obtained are σ_{app} of 87.53 Ω cm^2 s$^{-0.5}$ at the combination of 0.390Li–0.355Na–0.255K and a total pressure of 4.2 atm.

4. Conclusions

The effect of $O_2/CO_2 = 90/10$ gas mixtures on the diffusion resistance during oxygen reduction in carbonate

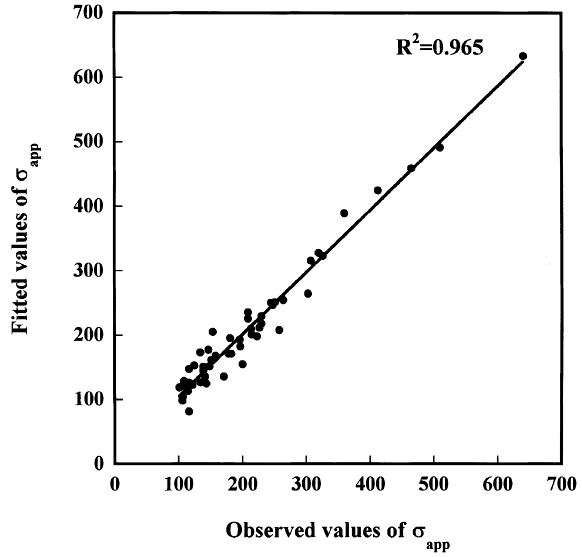

Fig. 7. Fitted σ_{app} values obtained with the partial cubic model against observed σ_{app} values.

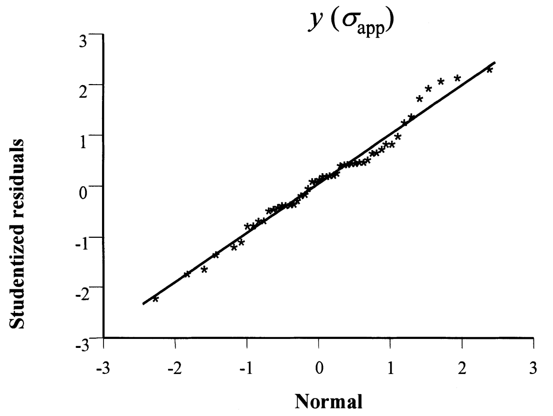

Fig. 8. Assessment of data adequacy by means of residuals plots. Studentized residuals against normal data.

Table 2. Assessment of the predictive power of the partial cubic model for a new input of electrolyte composition of 0.568Li–0.312Na–0.12K at various total pressures of O_2/CO_2 = 90/10 gas mixtures

Total pressure /atm	Experimental σ_{app} /Ω cm^2 s$^{-0.5}$	Predicted σ value	
		Mean value	Limits of confidence interval = 95%
1	330.3	385.16	326–444.3
3	143.2	200.27	141.72–258.82
5	136.5	168.82	103.71–233.93

melts of variable composition, ranging from the eutectics Li–K, Li–Na to ternary Li–Na–K melts, has been investigated under atmospheric and pressurized gas conditions. It was found that pressurization decreased the diffusion resistance of the reactant species in all melt compositions considered. This was attributed to an increase in the concentration of the reactive species in the electrolyte. Reaction order plots of Warburg coefficient against the total pressure in binary melts showed that: (i) mixed diffusion of superoxide ions and CO_2 dominates in lithium rich carbonates, and (ii) mixed diffusion of peroxide ions and CO_2 is preponderant in potassium rich carbonates.

Using the method of multivariate analysis, a partial cubic model was found to describe, with satisfactory accuracy, the relationship between a wide range of alkali carbonate compositions and oxygen solubility under pressurized conditions. Moreover, two optimum alkali carbonate compositions are proposed at atmospheric and under pressurized conditions of O_2/CO_2 = 90/10 gas mixtures.

The method used here does not require *a priori* knowledge of the investigated system, but generates a model based entirely on the collected data. Thus, the model is only valid within the experimental domain for which it was conducted. Using the model to predict data outside the experimental domain of reference measurement (i.e., extrapolation) is uncertain and should be avoided. The model gives no chemical information about the system, yet it is possible to use multivariate methods to achieve chemical information. This process is much more complicated and requires more fundamental knowledge about the system.

Acknowledgements

This work was supported by the Proposal-Based Immediate-Effect R&D Promotion Program 98Z31-011 from the New Energy and Industrial Technology Development Organization (NEDO). We are grateful to Professor Patrick Ozil for the initiation to the experimental design methodology.

References

1. J.R. Selman, 'Fuel Cell Systems' (Plenum Press, New York, 1993).
2. L. Plomp, E.F. Sitters, J.P. Hujismans and S.B. van der Molen, *in* Proceedings of the Second Symposium on 'Molten Carbonate Fuel Cell Technology', PV 90-16, The Electrochemical Society, Pennington, NJ (1990), p. 247.
3. L. Plomp, J.B.J. Veldhuis, E.F. Sitters and S.B. Van der Molen, *J. Power Sources* **39** (1992) 369.
4. L. Giorgi, M. Carewska, E. Simonetti, S. Scaccia, F. Croce and A. Pozio, *Molten Salt Forum* **1–2** (1993/94) 285.
5. K-K. Young and Y-B. Young, *Electrochim. Acta* **43** (1998) 3343.
6. L. Giorgi, A. Moreno, A. Pozio and E. Simonetti, *in* Proceedings the Fifth Symposium on 'Molten Carbonate Fuel Cell Technology', PV 99-20, The Electrochemical Society, Pennington, NJ (1999), p. 265.
7. C. Belhomme, E. Gourba, M. Cassir and C. Tessier, *J. Electroanal. Chem.* **503** (2001) 69.
8. M. Mohamedi, Y. Hisamitsu, K. Kihara, T. Kudo, T. Itoh and I. Uchida, *J. Alloys Comp.* **315** (2001) 224.
9. K. Ota, S. Mistushima, S. ato, H. Yoshitake and N. Kamiya, *J. Electrochem. Soc.* **139** (1992) 667.
10. J.R. Selman and H.C. Maru, *in* G. Mamantov and J. Braunstein (Eds), 'Advances in Molten Salt Chemistry', Vol. 4 (Plenum Press, New York, 1981), p. 159.
11. H. Mohn and H. Wendt, *Z. Physik. Chem.* **192** (1995) 101.
12. T. Nishina, I. Uchida and J.R. Selman, *J. Electrochem. Soc.* **141** (1994) 1191.

13. M. Mohamedi, Y. Hisamitsu, Y. Ono, T. Itoh and I. Uchida, *J. Appl. Electrochem.* **30** (2000) 1397.
14. I. Uchida, T. Nishina, Y. Mugikura and K. Itaya, *J. Electroanal. Chem.* **206** (1986) 229.
15. I. Uchida, Y. Mugikura, T. Nishina and K. Itaya, *J. Electroanal. Chem.* **206** (1986) 241.
16. I. Uchida, T. Nishina, Y. Mugikura and K. Itaya, *J. Electroanal. Chem.* **209** (1986) 125.
17. A.J. Appleby and S.B. Nicholson, *J. Electroanal. Chem.* **112** (1980) 71.
18. K. Yamada, T. Nishina, I. Uchida and J.R. Selman, *Electrochim. Acta* **38** (1993) 2405.
19. G.B. Dunks and D. Stelman, *Inorg. Chem.* **22** (1983) 2168.
20. R. Makkus, Doctoral thesis, Delft University of Technology, Delft (1991).
21. T. Itoh, Y. Hisamitsu, M. Mohamedi, M. Nishizawa, T. Abe, P. Tomczyk and I. Uchida, *Chem. Lett.* (1999) 1115.
22. G.E.P. Box, W.G. Hunter and J.S. Hunter, 'Statistics for Experimenters' (Wiley & Sons, New York, 1978).